Acta Crystallographica Section B
Structural Science
ISSN 0108-7681

Phase transitions in KTP isostructures: correlation between structure and T_c in germanium-doped $RbTiOPO_4$

Stefan T. Norberg,[a]* Joacim Gustafsson[a] and Bengt-Erik Mellander[b]

[a]Materials and Surface Chemistry, Chalmers University of Technology, SE-412 96 Göteborg, Sweden, and [b]Physics and Engineering Physics, Chalmers University of Technology, SE-412 96 Göteborg, Sweden

Correspondence e-mail: stn@inoc.chalmers.se

Received 28 April 2003
Accepted 2 September 2003

Crystals of germanium-doped rubidium titanyl phosphate, $Rb_2(Ti)(Ge_{0.121}Ti_{0.879})O_2(PO_4)_2$ (GeRTP#1) and $Rb_2(Ge_{0.125}Ti_{0.875})(Ge_{0.225}Ti_{0.775})O_2(PO_4)_2$ (GeRTP#2), have been structurally characterized from X-ray diffraction data at room temperature. In addition, a third structure, $Rb_2(TiO)_2(PO_4)_2$ (RTP), has been reinvestigated. The exchange of titanium for germanium results in a less distorted octahedral coordination around the two crystallographically independent titanium sites. Additionally, rubidium split-cation positions have been found in these doped RTP crystals. Dielectric measurements show that the phase-transition temperature, T_c, decreases with increasing germanium concentration, and a direct correlation between the room-temperature split of the rubidium cations and T_c has been discovered. General trends regarding the relationship between the room-temperature structures of KTP-like compounds and their T_c values are discussed.

1. Introduction

Rubidium titanyl phosphate ($RbTiOPO_4$, RTP; Thomas *et al.*, 1992) belongs to the $KTiOPO_4$ (KTP) family of structures. Since the structural determination by Tordjman *et al.* (1974), this family has become a well known class of materials for nonlinear optical applications (Bierlein, 1989; Stucky *et al.*, 1989). The properties of thermal stability, chemical resistivity, high nonlinearity and high optical damage threshold of KTP, as well as a wide optical transmission window, extend to RTP and some other common KTP isostructural compounds, which are best described as $ATiOBO_4$ compounds, with A = K, Rb, Cs or Tl, and B = P or As (Stucky *et al.*, 1989, and references therein).

The actual number of known KTP isostructures is much larger than the compounds covered by this definition, and a complete list would include many compounds with reduced or almost nonexistent nonlinear optical coefficients. For instance, it is possible to exchange the titanium and/or the alkaline metal completely or partly during the growth of KTP structures, *e.g.* $KSnOPO_4$ (Thomas *et al.*, 1990), $Sr_{0.06}K_{0.87}Cr_{0.05}Ti_{0.95}OPO_4$ (Norberg *et al.*, 2000) and $K_{0.59}Tl_{0.41}TiOPO_4$ (Voronkova *et al.*, 1994). KTP-like $AMOBO_4$ structures can, for instance, be formed by atomic combinations with A = K, Rb, Cs, Tl, Na, Ag or NH_4^+, M = Ti, Sn, Nb or Ge, and B = P or As, even if not all combinations yield single crystals. Nevertheless, the large number of KTP isostructural compounds

with different crystalline properties offers a valuable opportunity for the study of fundamental structurally related properties, such as pyroelectricity, ferroelectricity, nonlinear optical susceptibility and phase-transition temperature.

Ge-doped RTP crystals should be suitable for ferroelectric-to-paraelectric phase-transition studies. Previous studies have shown that the replacement of Ti by Ge in KTP crystals decreases the phase-transition temperature, T_c. KTP has a T_c value of 1207 K (Stefanovich *et al.*, 1996), while T_c is 1133 K for $KGe_{0.06}Ti_{0.94}OPO_4$ (Sorokina *et al.*, 1995) and 1058 K for completely Ge-exchanged KTP (Voronkova *et al.*, 1993), *i.e.* $KGeOPO_4$. The T_c value of 1062 K for $RbTiOPO_4$ (RTP; Stefanovich *et al.*, 1996) is already substantially lower than that for KTP, and it is likely that the introduction of Ge into RTP will decrease T_c further. It should, therefore, be possible to study potential effects on the atomic structure that are due to a decreased T_c value, and it may be possible to collect X-ray intensities at temperatures above T_c.

Small single crystals of $KGe_xTi_{1-x}OPO_4$ are grown easily by crystallization from melts in the K_2O–GeO_2/TiO_2–P_2O_5 system. Voronkova *et al.* (1993) have determined the atomic structure and ferroelectric phase transition of $KGeOPO_4$. Sorokina *et al.* (1995) investigated the structure and electrophysical properties of $KGe_{0.06}Ti_{0.94}OPO_4$. Single crystals of $KGe_{0.04}Ti_{0.96}OPO_4$ and $KGe_{0.18}Ti_{0.82}OPO_4$ were characterized by Sorokina *et al.* (1996). Flux growth of large $KGe_xTi_{1-x}O\backslash$-forcelb]PO_4 crystals by top-seeded solution growth has been accomplished by Nikolov *et al.* (1999).

Alkaline split-cation positions in KTP isostructures have drawn a considerable amount of attention, although there are few examples of split positions in $ATiOBO_4$ compounds with high nonlinear coefficients. Belokoneva *et al.* (1990) observed K split positions in $KFeFPO_4$ and mentioned the existence of a similar phenomenon in KTP. Split positions have also been found at room temperature in $CsTiOAsO_4$ (CTA; Nordborg, 2000), $RbTiOAsO_4$ (RTA; Streltsov *et al.*, 2000) and $Cs_xRb_{1-x}TiOAsO_4$ (Thomas & Womersley, 1998). The approach from non-centrosymmetry to centrosymmetry has been studied in RTP and KTP by Delarue *et al.* (1998, 1999) using X-ray diffraction data in the temperature range 293–973 K, *i.e.* below the actual T_c of these compounds. It was seen that alkaline split-cation positions appeared at temperatures above room temperature in both structures and that these positions increase in occupancy and displacement with increasing temperature. Models for the phase transitions of KTP isostructural compounds were further developed by Norberg *et al.* (2003), who demonstrated a possible correlation between the alkaline cation displacement along the polar *c* axis and the Abrahams–Jamieson–Kurtz (Abrahams, 1994) T_c criteria for ferroelectric oxygen-framework structures.

We have grown a series of Ge-doped RTP crystals, *i.e.* $RbGe_xTi_{1-x}OPO_4$ (RTP, GeRTP#1 and GeRTP#2, with $x = 0$, 0.06 and 0.17, respectively), in order to investigate the relationship between room-temperature atomic structure and T_c. We describe here how the appearance of alkaline split sites and their occupancies directly correlate with T_c in $ATiOBO_4$ compounds (A = K, Rb, Cs or Tl, and B = P or As).

2. Experimental

2.1. Crystallization

Single crystals of Ge-doped RTP were grown by spontaneous nucleation in self-fluxes, *i.e.* fluxes containing no elements other than those in the crystals. GeRTP#1 was crystallized from a batch containing Rb_2CO_3, $(NH_4)H_2PO_4$, TiO_2 and GeO_2 in a 2:3:0.75:0.25 molar ratio, and GeRTP#2 from a batch with a 2:3:0.63:0.37 molar ratio. The reagents were mixed thoroughly in 35 ml platinum crucibles, and the mixtures were heated slowly to 1373 K over a 3 d period and kept at this temperature for 48 h. The temperature was then lowered to 973 K at a rate of 1.85 K h^{-1}, and thereafter the mixtures were cooled quickly to room temperature. HCl (5 *M*) was used to dissolve the fluxes. All crystals obtained were transparent and colourless, with sizes ranging from a few micrometres to ~2 mm. No crystallization occurred in fluxes with a Ti/Ge ratio smaller than that of the GeRTP#2 flux.

RTP single crystals were grown by spontaneous crystallization in a batch containing TiO_2, Rb_2CO_3 and $(NH_4)H_2PO_4$ in a 1:2:3 molar ratio. The batch was mixed in a platinum crucible, and then heated to 1273 K for a period of 4 d, kept at that temperature for 60 h, cooled to 1023 K at a rate of 1.4 K h^{-1} and thereafter cooled quickly to room temperature. The flux dissolved in water, and transparent colourless crystals of sizes ranging from a few micrometres to a couple of millimetres were obtained. Many of the smaller crystals had the typical KTP morphology (Bolt & Bennema, 1990).

The Ti/Ge ratio in crystals from the GeRTP#2 flux was analysed by energy-dispersive X-ray measurements (electroscan S4-8DV equipped with a Link eX1 EDX system). The chosen crystals were of similar size and morphology to the crystal used for structural determination. All measurements indicated a Ti/Ge ratio of ~5:1, and this closely resembles the ratio determined by the refinement of X-ray diffraction data.

2.2. Data collection

X-ray intensities for all crystals were collected with a Siemens SMART CCD diffractometer (Siemens, 1995) using Mo $K\alpha$ radiation at room temperature. Data were collected by ω scans, advancing 0.3° for each collected frame. The crystal-to-detector distance was 3.97 cm and the CCD detector was held at $2\theta = -32°$. Collected frames were integrated with *SAINT* (Siemens, 1995) and absorption corrections were performed empirically by *SADABS* (Sheldrick, 2001). The final cell measurements were carried out with an Enraf–Nonius CAD-4 diffractometer and refined with diffractometer software (Enraf–Nonius, 1989). Symmetry-equivalent reflections were averaged while keeping Friedel mates separated. Further details concerning data collection and refinement can be found in Table 1.[1]

[1] Supplementary data for this paper are available from the IUCr electronic archives (Reference: OS0109). Services for accessing these data are described at the back of the journal.

Table 1
Experimental details.

	RTP	GeRTP#1	GeRTP#2
Crystal data			
Chemical formula	$Rb_2(TiO)_2(PO_4)_2$	$Rb_2(Ti)(Ge_{0.121}Ti_{0.879})O_2(PO_4)_2$	$Rb_2(Ge_{0.125}Ti_{0.875})(Ge_{0.225}Ti_{0.775})O_2(PO_4)_2$
M_r	488.64	491.62	497.28
Cell setting, space group	Orthorhombic, $Pna2_1$	Orthorhombic, $Pna2_1$	Orthorhombic, $Pna2_1$
a, b, c (Å)	12.9625 (15), 6.5031 (3), 10.5615 (3)	12.9386 (18), 6.5085 (8), 10.4408 (10)	12.9179 (12), 6.5189 (8), 10.3633 (14)
V (Å^3)	890.30 (11)	879.23 (18)	872.70 (18)
Z	4	4	4
D_x (Mg m^{-3})	3.645	3.714	3.785
Radiation type	Mo $K\alpha$	Mo $K\alpha$	Mo $K\alpha$
No. of reflections for cell parameters	18	23	19
θ range (°)	17.9–23.9	19.6–27.3	16.3–29.6
μ (mm^{-1})	13.06	13.53	14.21
Temperature (K)	293 (2)	293 (2)	293 (2)
Crystal form, colour	Rectangle, colourless	Rectangle, colourless	Rectangle, colourless
Crystal size (mm)	0.14 × 0.12 × 0.08	0.60 × 0.10 × 0.04	0.10 × 0.05 × 0.04
Data collection			
Diffractometer	Siemens SMART CCD	Siemens SMART CCD	Siemens SMART CCD
Data collection method	ω scans	ω scans	ω scans
Absorption correction	Multi-scan (*SADABS*; Sheldrick, 2001)	Multi-scan (*SADABS*; Sheldrick, 2001)	Multi-scan (*SADABS*; Sheldrick, 2001)
T_{min}	0.175	0.207	0.421
T_{max}	0.353	0.578	0.564
No. of measured, independent and observed reflections	10 947, 2054, 2054	12 286, 2513, 2513	12 604, 2497, 2497
Criterion for used reflections	$F > 0\sigma(F)$	$F > 0\sigma(F)$	$F > 0\sigma(F)$
R_{int}	0.052	0.031	0.039
θ_{max} (°)	27.5	29.8	29.8
Range of h, k, l	$-16 \Rightarrow h \Rightarrow 16$ $-8 \Rightarrow k \Rightarrow 8$ $-13 \Rightarrow l \Rightarrow 13$	$-18 \Rightarrow h \Rightarrow 18$ $-9 \Rightarrow k \Rightarrow 9$ $-14 \Rightarrow l \Rightarrow 14$	$-18 \Rightarrow h \Rightarrow 18$ $-9 \Rightarrow k \Rightarrow 9$ $-14 \Rightarrow l \Rightarrow 14$
Refinement			
Refinement on	F	F	F
$R[F > 2\sigma(F)]$, $wR(F)$, S	0.024, 0.037, 1.13	0.021, 0.032, 1.05	0.025, 0.039, 1.04
No. of reflections	2054	2513	2497
No. of parameters	146	158	156
Weighting scheme	$w = 1/(\sigma^2F + 0.002F^2)$	$w = 1/(\sigma^2F + 0.0015F^2)$	$w = 1/(\sigma^2F + 0.002F^2)$
$(\Delta/\sigma)_{max}$	0.001	<0.001	0.001
$\Delta\rho_{max}$, $\Delta\rho_{min}$ (e Å^{-3})	1.11, −0.71	0.61, −0.60	0.73, −0.91
Extinction method	Isotropic Gaussian	Isotropic Gaussian	None
Extinction coefficient	117 (5) × 10^2	4 (1) × 10^2	–
Absolute structure	Flack (1983)	Flack (1983)	Flack (1983)
Flack parameter	0.497 (9)	0.429 (8)	0.487 (11)

Computer programs: *SMART* (Siemens, 1995), *CAD*-4 *Software* (Enraf–Nonius, 1989), *SAINT* (Siemens, 1995), *SADABS* (Sheldrick, 2001), *CRYLSQ*, *BONDLA*, *ATABLE* and *CIFIO* in *Xtal*3.71 (Hall *et al.*, 2000), *ORTEP*-3 *for Windows* (Farrugia, 1997). Atomic parameters from Norberg *et al.* (2000).

2.3. Structure refinement

The structures of both Ge-doped RTP compounds were refined using the *Xtal*3.71 software package (Hall *et al.*, 2000). The first cycles of refinement for GeRTP#1 were carried out without any dopant, using atomic parameters from Norberg *et al.* (2000), and converged to $R = 0.030$, $wR = 0.043$ and $S = 1.389$, with $\Delta\rho_{max}$ and $\Delta\rho_{min}$ of 2.47 and −0.90 e Å^{-3} [$\sigma(\Delta\rho) = 0.08$ e Å^{-3}]. The residual electron-density maps showed two significant high peaks in the vicinity of atoms Rb1 and Rb2, with peak-to-Rb distances of 0.768 (1) and 0.655 (1) Å, respectively. These positions were described as Rb split-cation positions in subsequent refinements, and all atomic positions were refined with anisotropic displacement parameters, which resulted in $R = 0.024$, $wR = 0.036$, $S = 1.179$, $\Delta\rho_{max} = 1.02$ e Å^{-3} and $\Delta\rho_{min} = -0.82$ e Å^{-3} [$\sigma(\Delta\rho) = 0.08$ e Å^{-3}]. One remaining peak of significant residual electron density was found in the vicinity of atom Ti2. It was also noted that the U_{eq}(Ti2) value was small compared with U_{eq}(Ti1). The peak of excess electron density was described for further refinements as the Ge dopant. The final refinement with both Ge dopant and Rb split-cation positions resulted in the structure and parameters given in Table 1 [$\sigma(\Delta\rho) = 0.08$ e Å^{-3}].

An isotropic extinction parameter (Zachariasen, 1967) using Larson's implementation (Larson, 1970) was refined for the GeRTP#1 structure, and 3.8% of the reflections were affected by extinction. The maximum correction of $y = 0.95$ was used for the 013 and 203 reflections (the observed struc-

ture factor is $F_{obs} = yF_{kin}$, where F_{kin} is the kinematic value). The Flack (1983) parameter refined to 0.429 (8), which indicates that the crystal contained a mixture of domains with opposite polarization, *i.e.* approximately 43% of the [001] inversion twin.

GeRTP#2 was refined in a similar way using atomic parameters from Norberg *et al.* (2000), and the refinement converged to $R = 0.045$, $wR = 0.063$, $S = 1.678$, $\Delta\rho_{max} = 3.54$ e Å^{-3} and $\Delta\rho_{min} = -1.52$ e Å^{-3} [$\sigma(\Delta\rho) = 0.12$ e Å^{-3}]. Analysis of the residual electron-density peaks indicated extra Rb sites at distances of 0.809 (3) and 0.887 (3) Å from the Rb1 and Rb2 sites. This structural model refined to $R = 0.035$, $wR = 0.052$, $S = 1.397$, $\Delta\rho_{max} = 1.47$ e Å^{-3} and $\Delta\rho_{min} = -1.42$ e Å^{-3} [$\sigma(\Delta\rho) = 0.12$ e Å^{-3}]. In the resulting structural model, the U_{eq}(Ti1) value is twice as large as U_{eq}(Ti2), thus indicating Ge-atom inclusion close to atom Ti2. Refinement with a Ge atom at the Ti2 site resulted in a single peak of residual electron density around the Ti1 site, thus indicating a likely Ge-atom inclusion at that site. Refinement with mixed Ti/Ge populations at both Ti sites resulted in the structure and parameters given in Table 1 [$\sigma(\Delta\rho) = 0.13$ e Å^{-3}]. No extinction parameter was refined for the small GeRTP#2 crystal, and the Flack (1983) parameter refined to 0.487 (11), which is similar to the the value obtained for the GeRTP#1 structure.

The structure of RTP was refined in the same way as the Ge-doped RTP structures. There were slight indications of low occupancy split-cation positions along the polar *c* direction, but these could not be refined. The structural parameters coincide well with those determined by Thomas *et al.* (1992). Details regarding the refinement of RTP are given in Table 1.

Atomic fractional coordinates and occupation and displacement parameters for $RbTiOPO_4$, $RbGe_{0.06}Ti_{0.94}OPO_4$ and $RbGe_{0.17}Ti_{0.83}OPO_4$ are given in the supplementary material, together with the calculated and observed structure factors.

2.4. Dielectric measurements

Electrical properties were measured *via* impedance spectroscopy on pressed cylindrical samples of RTP and GeRTP#1 powder, approximately 1.5 mm thick and 8 mm in diameter. The samples were pressed and then sintered at 1273 K for 24 h in aluminium oxide crucibles. Platinum paint was then applied to the top and bottom surfaces of the tablets, and they were heated to 1173 K. Complex impedance measurements at frequencies of between 5 Hz and 13 MHz were performed using a computerized HP 4192 A impedance analyser. The applied signal was 100 mV and the measurements were carried out in the temperature range 298–1173 K using a thermostated sample cell.

3. Result and discussion

3.1. Structure and dopant inclusion

Both GeRTP#1 and GeRTP#2 have a structural network (Fig. 1) with bond distances (Table 2) similar to those of RTP (Thomas *et al.*, 1992) and are thus isostructural to KTP (Tordjman *et al.*, 1974). The crystals consist of two crystallographically independent TiO_6 octahedra, which are distorted and linked together by corner sharing (alternately *cis* and *trans*), thus forming helical chains throughout the structure. Both octahedra have one short and one long Ti—O bond, and these take part in the helical chain as –Ti1—O11—Ti2—O12– sequences. This part of the structure is believed to be important for the nonlinear properties of these materials. The TiO_6 octahedra are further bridged by PO_4 tetrahedra, in such a way that large structural cages occupied by loosely bonded rubidium cations are created. These cation cavities are connected by channels along the polar *c* axis, which give rise to a highly anisotropic ionic conductivity.

The exchange of Ti for Ge results in changes to the RTP lattice parameters. The *a* and *c* axes are shortened with increased Ge content, whereas the *b* axis becomes slightly

Table 2
Selected interatomic distances (Å) for RTP, GeRTP#1 and GeRTP#2.

	$RbTiOPO_4$	GeRTP#1	GeRTP#2
Rb1*a*—O1	3.037 (4)	3.082 (4)	3.098 (7)
Rb1*a*—O2	2.740 (4)	2.728 (4)	2.720 (7)
Rb1*a*—O3^{i}	2.773 (4)	2.773 (3)	2.771 (5)
Rb1*a*—O11	3.171 (4)	3.228 (4)	3.277 (7)
Rb1*a*—O12^{i}	2.790 (4)	2.783 (3)	2.776 (6)
Rb1*a*—O5^{i}	2.998 (4)	3.021 (5)	3.055 (7)
Rb1*a*—O6^{iii}	3.400 (4)	3.327 (4)	3.281 (6)
Rb1*a*—O7^{i}	3.220 (4)	3.260 (4)	3.295 (7)
Rb1*a*—O8	2.841 (5)	2.828 (13)	2.818 (6)
Rb1*b*—O2		2.675 (9)	2.682 (11)
Rb1*b*—O3^{i}		2.865 (10)	2.886 (12)
Rb1*b*—O12^{i}		2.753 (9)	2.751 (10)
Rb1*b*—O6^{iii}		3.026 (10)	2.996 (12)
Rb1*b*—O8		2.850 (9)	2.842 (11)
Rb2*a*—O1^{iv}	2.749 (4)	2.737 (4)	2.725 (6)
Rb2*a*—O2^{ii}	3.107 (4)	3.113 (4)	3.130 (7)
Rb2*a*—O3^{ii}	3.120 (4)	3.116 (5)	3.147 (8)
Rb2*a*—O4^{v}	3.043 (4)	3.020 (4)	2.995 (5)
Rb2*a*—O11	2.791 (4)	2.780 (3)	2.773 (6)
Rb2*a*—O12^{ii}	3.110 (4)	3.128 (4)	3.149 (6)
Rb2*a*—O5^{vi}	2.863 (4)	2.859 (3)	2.866 (5)
Rb2*a*—O7^{ii}	3.000 (4)	2.974 (4)	2.950 (7)
Rb2*a*—O8^{ii}	3.127 (8)	3.15 (3)	3.184 (7)
Rb2*b*—O1^{iv}		2.652 (13)	2.632 (16)
Rb2*b*—O4^{v}		2.83 (2)	2.792 (19)
Rb2*b*—O11		2.701 (13)	2.706 (16)
Rb2*b*—O5^{vi}		2.988 (16)	3.067 (18)
Rb2*b*—O7^{ii}		2.882 (13)	2.837 (16)
Ti1—O1	2.127 (4)	2.094 (4)	2.058 (7)
Ti1—O2^{vii}	1.957 (4)	1.964 (4)	1.973 (7)
Ti1—O11	1.964 (4)	1.902 (4)	1.856 (6)
Ti1—O12^{ii}	1.723 (4)	1.755 (4)	1.785 (6)
Ti1—O5^{ii}	2.083 (4)	2.095 (4)	2.090 (5)
Ti1—O6^{viii}	2.027 (4)	2.025 (3)	2.030 (6)
Ti2—O3	2.059 (4)	2.077 (6)	2.051 (4)
Ti2—O4^{v}	2.015 (4)	1.982 (6)	2.003 (4)
Ti2—O11	1.740 (4)	1.764 (7)	1.816 (7)
Ti2—O12	2.087 (4)	2.011 (7)	1.927 (7)
Ti2—O7^{viii}	1.962 (4)	1.956 (4)	1.942 (7)
Ti2—O8	2.000 (10)	1.95 (4)	1.947 (7)

Symmetry codes: (i) $x, 1+y, z$; (ii) $\frac{3}{2}-x, \frac{1}{2}+y, \frac{1}{2}+z$; (iii) $x-\frac{1}{2}, \frac{3}{2}-y, z$; (iv) $\frac{1}{2}+x, \frac{3}{2}-y, z$; (v) $\frac{1}{2}+x, \frac{1}{2}-y, z$; (vi) $2-x, 1-y, \frac{1}{2}+z$; (vii) $1-x, 1-y, \frac{1}{2}+z$; (viii) $\frac{3}{2}-x, y-\frac{1}{2}, \frac{1}{2}+z$.

Table 3
Lattice parameters for $KGe_xTi_{1-x}OPO_4$ and $RbGe_xTi_{1-x}OPO_4$ structures.

	a (Å)	*b* (Å)	*c* (Å)	*V* (Å^3)	References
$KTiOPO_4$	12.819 (3)	6.399 (1)	10.584 (2)	868.2 (3)	Thomas *et al.* (1990)
$KGe_{0.04}Ti_{0.96}OPO_4$	12.7788 (15)	6.4002 (6)	10.5268 (10)	860.95 (14)	Sorokina *et al.* (1996)
$KGe_{0.06}Ti_{0.94}OPO_4$	12.7633 (10)	6.3992 (5)	10.4988 (13)	857.49 (14)	Sorokina *et al.* (1995)
$KGe_{0.18}Ti_{0.82}OPO_4$	12.7252 (16)	6.3944 (7)	10.4212 (20)	848.0 (2)	Sorokina *et al.* (1996)
KGeOPO4	12.6013 (10)	6.3051 (5)	10.0031 (8)	794.77 (11)	Voronkova *et al.* (1993)
$RbTiOPO_4$	12.9625 (15)	6.5031 (3)	10.5615 (3)	890.30 (11)	This report
$RbGe_{0.06}Ti_{0.94}OPO_4$	12.9386 (18)	6.5085 (8)	10.4408 (10)	879.23 (18)	This report
$RbGe_{0.17}Ti_{0.83}OPO_4$	12.9179 (12)	6.5189 (8)	10.3633 (14)	872.70 (18)	This report

longer. This behaviour follows the trends found in Ge-doped KTP (Sorokina *et al.*, 1995, 1996), in which both *a* and *c* axes decreased with increasing Ge content, while only a miniscule decrease of the *b* axis was noted (see Table 3). There is a clear preference for the Ge atom to be positioned in the slightly less distorted $Ti2O_6$ octahedron in both GeRTP#1 and GeRTP#2. All of the Ge atoms in GeRTP#1 and about two-thirds of the Ge atoms in GeRTP#2 are situated in the $Ti2O_6$ octahedron. Both TiO_6 octahedra also become significantly less distorted as Ge replaces Ti, as can be seen in Table 4 and Fig. 2. All major changes in Ti—O bond distances take place in the Ti1—O11/O12 and Ti2—O11/O12 bonds. The effect is most significant in the $Ti2O_6$ octahedron, which has a higher concentration of Ge. The Ti2—O12 bond is, for instance, the longest bond in its octahedron in RTP but the second shortest bond in GeRTP#2. It should be noted that atoms Ge2 and Ti2 are separated by 0.18 (2) Å in GeRTP#1 while they coincide in GeRTP#2. This difference is due to the greater distortion of the Ti2—O11/O12 bonds in GeRTP#1. The Ge2—O11/O12 bond distances in GeRTP#1 are 1.89 (2) and 1.88 (2) Å, respectively, while the corresponding Ti2—O11/O12 bond distances are 1.764 (7) and 2.011 (7) Å, respectively.

There are no significant differences between bond distances in the PO_4 tetrahedra of RTP, GeRTP#1 and GeRTP#2. GeRTP#1 has P—O bond distances that range from 1.521 (5)

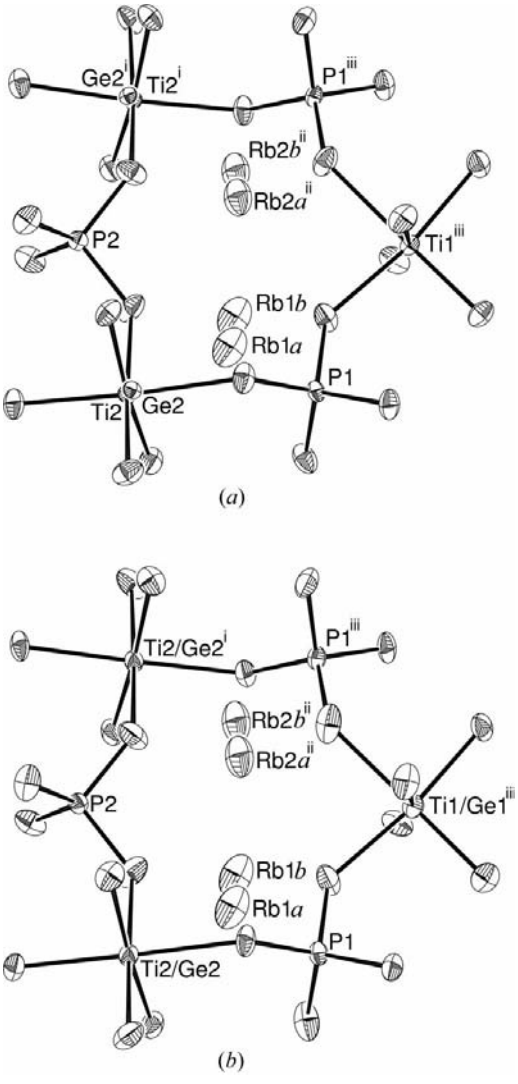

Figure 1
Ellipsoid plots of the (*a*) $RbGe_{0.06}Ti_{0.94}OPO_4$ and (*b*) $RbGe_{0.17}Ti_{0.83}OPO_4$ structures projected on the (010) plane. Displacement ellipsoids are drawn at the 80% probability level. [Symmetry codes: (i) $\frac{3}{2}-x$, $y+\frac{1}{2}$, $z-\frac{1}{2}$; (ii) $1-x$, $1-y$, $z-\frac{1}{2}$; (iii) $-\frac{3}{2}-x$, $y-\frac{1}{2}$, $z-\frac{1}{2}$].

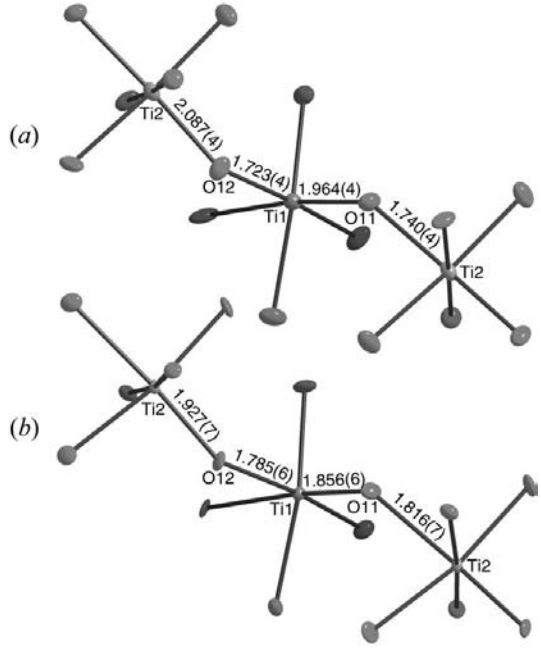

Figure 2
The –Ti2—O12—Ti1—O11—Ti2– sequence in (*a*) RTP and (*b*) GeRTP#2.

Table 4
Geometric changes (Å) to the Ti/GeO_6 octahedra for $RbGe_xTi_{1-x}OPO_4$ compounds.

	$RbTiOPO_4$	$RbGe_{0.06}Ti_{0.94}OPO_4$	$RbGe_{0.17}Ti_{0.83}OPO_4$
$(Ti1-O)_{max}$	2.127 (4)	2.095 (4)	2.090 (5)
$(Ti1-O)_{min}$	1.723 (4)	1.755 (4)	1.785 (6)
$\Delta(Ti1-O)$	0.40	0.34	0.31
$(Ti2-O)_{max}$	2.087 (4)	2.077 (6)	2.051 (4)
$(Ti2-O)_{min}$	1.740 (4)	1.764 (7)	1.816 (7)
$\Delta(Ti2-O)$	0.35	0.31	0.24

to 1.548 (5) Å, while they range from 1.521 (8) to 1.546 (5) Å for GeRTP#2. The bond angles range from 105.5 (11) to 112.2 (3)°, with no significant differences for the two compounds. These values all resemble those in RTP, which has P—O bond distances in the range 1.526 (4)–1.550 (4) Å and bond angles of 105.6 (2)–111.6 (2)°.

The most significant difference between Ge-doped RTP and non-doped RTP is that the former structures have multiple rubidium cation sites along the polar *c* axis. GeRTP#1 and GeRTP#2 have similar structures, even if the distances between the original Rb site and the new alkaline sites are slightly longer in GeRTP#2 and the sites are of higher occupancy. The separation of the Rb1*a* and Rb1*b* atomic sites is 0.553 (17) Å in GeRTP#1, while the atomic sites of Rb2*a* and Rb2*b* are separated by 0.45 (4) Å. These distances are 0.57 (2) and 0.60 (3) Å in GeRTP#2. All of these Rb sites (see Fig. 3) have roughly the same coordination polyhedra in both GeRTP#1 and GeRTP#2.

3.2. Alkaline split positions and phase-transition temperatures

The ferroelectric-to-paraelectric phase transition in KTP isomorphs is recognized as a continuous second-order transition of both displacive and order–disorder type (Belokoneva *et al.*, 1997). The displacive part involves small changes in the structural framework of TiO_6 octahedra and PO_4 tetrahedra, while the order–disorder part involves quite substantial shifts of the alkaline cations within the cavities. These cavities contain, in addition to the alkaline cation site, a hole position, depicted in Fig. 3, to which the alkaline cation moves during polarization reversal induced by an electric field or the slower ferroelectric-to-paraelectric phase transition that is temperature driven.

Polarization reversal of the ferroelectric state involves a complete shift of all alkaline cations to the alternative hole positions, a process that most likely involves alkaline cation hopping instead of a continuous cation movement. In contrast, the slow process of ferroelectric-to-paraelectric phase transition involves both alkaline cation shifts and hopping towards new atomic sites. Both alkaline cations move along the polar *c* axis, as depicted for KTP in Figs. 4 and 5 (Norberg *et al.*, 2003), and the split-cation positions appear at an elevated temperature. This phenomenon should occur for all $ATiOBO_4$ (A = K, Rb, Cs or Tl, and B = P or As) compounds. It is also likely that $ATiOBO_4$ compounds with a T_c value substantially lower than

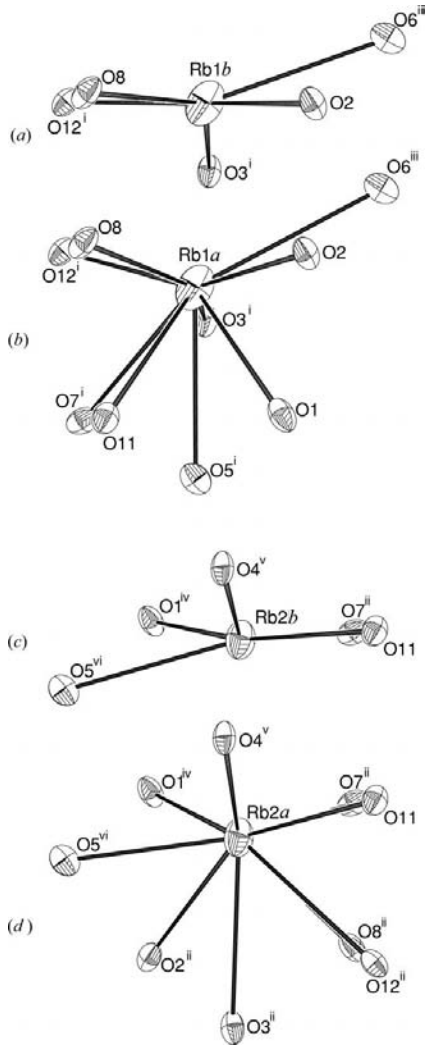

Figure 3
Views of the (*a*) Rb1*b*, (*b*) Rb1*a*, (*c*) Rb2*b* and (*d*) Rb2*a* cation–oxygen coordination in $RbGe_{0.06}Ti_{0.94}OPO_4$. Displacement ellipsoids are as in Fig. 1, and symmetry codes are as in Table 2.

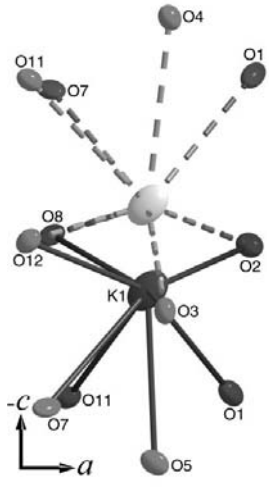

Figure 4
View of the K1 cavity, with a light-coloured atom situated at the hole site that correlates with the K1 atomic site.

that of KTP could have alkaline split positions at room temperature. This is indeed the case, as the recent structural characterizations of RTA (Streltsov *et al.*, 2000) and CTA (Nordborg, 2000) have shown, even though the implication of the alkaline split positions was not discussed in those papers.

Dopant inclusions (such as, for instance, an exchange of Ti for Sn, Ge or Nb) result in changes of T_c. These changes could in some cases be discovered by the appearance or disappearance of alkaline split-cation sites or from changes in the occupancy. Alkaline split sites should, in fact, be more pronounced the closer the structure is to the ferroelectric-to-paraelectric phase transition. The numerous investigations of the RTP structure (Thomas *et al.*, 1992; Delarue *et al.*, 1998; this report) clearly indicate that there are no alkaline split positions in the RTP structure at room temperature. Therefore, those positions discovered in the structure of our Ge-doped RTP indicate that the T_c values of GeRTP#1 and GeRTP#2 should be below that of RTP.

Our dielectric measurements on RTP and GeRTP#1 were performed over a wide frequency range in order to evaluate the static dielectric constant, ε_r. For insulating materials, this process is uncomplicated, since ε_r corresponds to the real part of the permittivity at low frequencies. In materials with a non-negligible electrical conductivity, the real part of the permittivity increases sharply at low frequencies because of polarization at the blocking electrodes. To avoid these effects, the value is usually obtained at intermediate frequencies, in our case at 100 kHz, which is above the range of electrode polarization effects but below the range of high-frequency relaxations that unavoidably occur at very high frequencies. Our measurements of RTP show a distinct peak at ~1075 K, in good agreement with the value published by Stefanovich *et al.* (1996). For the GeRTP#1 sample, the ε_r values increase in a similar way to those of RTP, but this increase occurs at a considerably lower temperature (see Fig. 6). There is a peak in ε_r at ~994 K, which we assign as T_c. This peak is not as sharp as that of RTP and, furthermore, at higher temperatures the ε_r values again increase. These effects are due to the conductivity

Table 5
Alkaline split sites at room temperature and values of T_c for some KTP isostructures.

The alkaline atomic sites are given in the format [occupancy for original site/occupancy for split site; distance between sites].

	Alkaline split sites		T_c (K)	References
$KTiOPO_4$	No	–	1207	Thomas *et al.* (1990) and Stefanovich *et al.* (1996)
$KGe_{0.04}Ti_{0.96}OPO_4$	No	–	–	Sorokina *et al.* (1996)
$KGe_{0.06}Ti_{0.94}OPO_4$	No	–	1133	Sorokina *et al.* (1995)
$KGe_{0.18}Ti_{0.82}OPO_4$	No	–	–	Sorokina *et al.* (1996)
KGeOPO4	No	–	1058	Voronkova *et al.* (1993)
$RbTiOPO_4$	No	–	1062	Thomas *et al.* (1992), Stefanovich *et al.* (1996), Delarue *et al.* (1998) and this report
$RbGe_{0.06}Ti_{0.94}OPO_4$	Yes	Rb1 [0.93/0.07; 0.553 (17) Å] Rb2 [0.94/0.06; 0.45 (4) Å]	994	This report
$RbGe_{0.17}Ti_{0.83}OPO_4$	Yes	Rb1 [0.88/0.12; 0.57 (2) Å] Rb2 [0.94/0.06; 0.60 (3) Å]	–	This report
$RbTiOAsO_4$	Yes	Rb1 [0.88/0.12; 0.312 (3) Å] Rb2 [0.87/0.13; 0.233 (4) Å]	1073	Streltsov *et al.* (2000) and Marnier *et al.* (1989)
$CsTiOAsO_4$	Yes	Cs1 [0.80/0.20; 0.366 (8) Å] Cs2 [0.80/0.20; 0.26 (2) Å]	943	Nordborg (2000) and Marnier *et al.* (1989)

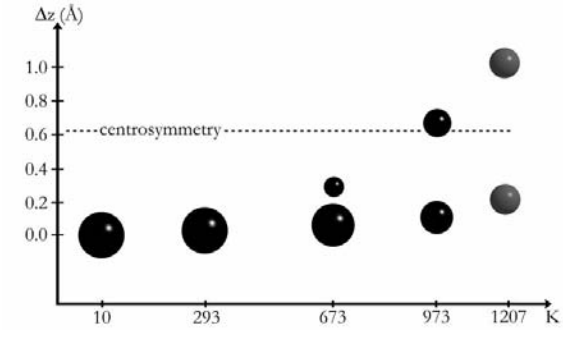

Figure 5
Alkaline displacement in KTP isostructures; the relative Δz (Å) shift is plotted *versus* the crystal temperature (K). The atomic size represents the occupancy parameter at each respective site. The two atoms at 1207 K show the likely split-cation positions for KTP at the ferroelectric-to-paraelectric phase transition.

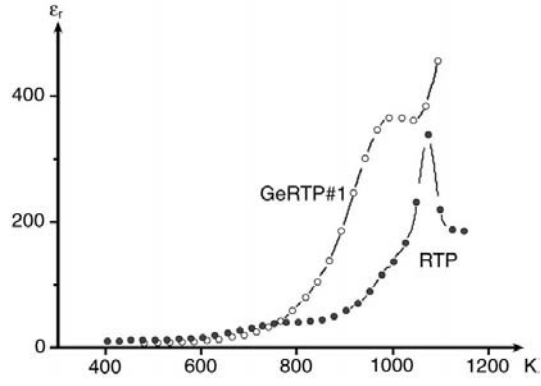

Figure 6
ε_r measured at 100 kHz for RTP (filled circles) and GeRTP#1 (open circles).

being higher in GeRTP#1 than in RTP, which leads to an apparent increase of the ε_r values at high temperature.

The lower T_c for GeRTP#1 is in agreement with that reported for $KGe_{0.06}Ti_{0.94}OPO_4$ (see Table 5). The main difference between the Ge-doped KTP structures and those of RTP is that there are no K split sites in the former structures, while Rb split sites have appeared in the latter structures. This difference could be expected, since all Ge-doped KTP structures have a T_c that is well above that of RTP. GeRTP#2 has larger occupancies on the Rb split sites and longer distances between the original sites and their split sites than GeRTP#1. GeRTP#2 should therefore have a T_c value below that of GeRTP#1.

The present investigation is the first of a series studying similar KTP isostructural compounds, in which the structures reveal information about the compounds' T_c values, thus making it possible to see if a certain compound is closer to the paraelectric state. It might even be possible to calibrate the behaviour of the alkaline cations and their room-temperature structures to their T_c values. It is, however, not possible to make this type of comparison for all kinds of KTP isostructures in order to predict values of T_c. General trends can be seen, but the different types of KTP isostructures, *e.g.* phosphates and arsenates, need to be separated. RTP and RTA have approximately the same T_c and only the latter compound has a structure with alkaline split-cation sites. Nevertheless, the increased distance between the alkaline split-cation sites and the increased occupancy of these sites in CTA (T_c = 943 K) compared with RTA (T_c = 1067 K) shows that the same trend exists for the arsenates.

Financial support from the Swedish Research Council is gratefully acknowledged. The authors are indebted to Professor Jörgen Albertsson and Dr Göran Svensson for helpful discussions, and to Dr Vratislav Langer for access to the SMART diffractometer and assistance in data collection.

References

Abrahams, S. C. (1994). *Acta Cryst.* A**50**, 658–685.
Belokoneva, E. L., Knight, K. S., Davids, W. I. F. & Mill, B. V. (1997). *J. Phys. Condens. Matter*, **9**, 3833–3851.
Belokoneva, E. L., Yakubovich, O. V., Tsirelson, V. G. & Urusov, V. S. (1990). *Izv. Akad. Nauk SSSR Neorg. Mater.* **26**, 595–601.
Bierlein, J. D. (1989). *SPIE Int. Soc. Opt. Eng.* **1104**, 2–11.
Bolt, R. J. & Bennema, P. (1990). *J. Cryst. Growth*, **102**, 329–340.
Delarue, P., Lecomte, C., Jannin, M., Marnier, G. & Menaert, B. (1998). *Phys. Rev. B*, **58**, 5287–5295.
Delarue, P., Lecomte, C., Jannin, M., Marnier, G. & Menaert, B. (1999). *J. Phys. Condens. Matter*, **11**, 4123–4134.
Enraf–Nonius (1989). *CAD*-4 *Software*, Version 5.0. Enraf–Nonius, Delft, The Netherlands.
Farrugia, L. J. (1997). *J. Appl. Cryst.* **30**, 565.
Flack, H. D. (1983). *Acta Cryst.* A**39**, 876–881.
Hall, S. R., du Boulay, D. J. & Olthof-Hazekamp, R. (2000). Editors. *Xtal*3.71. University of Western Australia, Australia.
Larson, A. C. (1970). *Crystallographic Computing*, edited by F. R. Ahmed, S. R. Hall & C. P. Huber, pp. 291–294. Copenhagen: Munksgaard.
Marnier, G., Boulanger, B. & Menaert, B. (1989). *J. Phys. Condens. Matter*, **1**, 5509–5513.
Nikolov, V., Koseva, I., Peshev, P., Solans, X., Solé, R., Ruiz, X., Gavalda, J., Massons, J., Aguiló, M. & Díaz, F. (1999). *Mater. Res. Bull.* **34**, 1403–1409.
Norberg, S. T., Sobolev, A. N. & Streltsov, V. A. (2003). *Acta Cryst.* B**59**, 353–360.
Norberg, S. T., Streltsov, V. A., Svensson, G. & Albertsson, J. (2000). *Acta Cryst.* B**56**, 980–987.
Nordborg, J. (2000). *Acta Cryst.* C**56**, 518–520.
Sheldrick, G. M. (2001). *SADABS*. Version 2.03. University of Göttingen, Germany.
Siemens (1995). *SMART* and *SAINT*. Siemens Analytical X-ray Instruments Inc., Madison, Wisconsin, USA.
Sorokina, N. I., Voronkova, V. I., Yanovskii, V. K., Verin, I. A. & Simonov, V. I. (1995). *Crystallogr. Rep.* **40**, 636–639.
Sorokina, N. I., Voronkova, V. I., Yanovskii, V. K., Verin, I. A. & Simonov, V. I. (1996). *Crystallogr. Rep.* **41**, 432–435.
Stefanovich, S., Mosunov, A., Mill, B. & Belokoneva, E. (1996). *Ferroelectrics*, **185**, 63–66.
Streltsov, V. A., Nordborg, J. & Albertsson, J. (2000). *Acta Cryst.* B**56**, 785–792.
Stucky, G. D., Phillips, M. L. F. & Gier, T. E. (1989). *Chem. Mater.* **1**, 492–509.
Thomas, P. A., Glazer, A. M. & Watts, B. E. (1990). *Acta Cryst.* B**46**, 333–343.
Thomas, P. A., Mayo, S. C. & Watts, B. E. (1992). *Acta Cryst.* B**48**, 401–407.
Thomas, P. A. & Womersley, M. N. (1998). *Acta Cryst.* B**54**, 645–651.
Tordjman, I., Masse, R. & Guitel, J. C. (1974). *Z. Kristallogr.* **139**, 103–115.
Voronkova, V. I., Yanovskii, V. K., Lee, D. Y., Sorokina, N. I., Verin, I. A., Furmanova, N. G. & Simonov, V. I. (1994). *Crystallogr. Rep.* **39**, 374–377.
Voronkova, V. I., Yanovskii, V. K., Sorokina, N. I., Verin, I. A. & Simonov, V. I. (1993). *Crystallogr. Rep.* **38**, 662–664.
Zachariasen, W. H. (1967). *Acta Cryst.* **23**, 558–564.